

1 SpiDa-MRI, behavioral and (f)MRI data of adults with fear of spiders

2 Authors

3 Mengfan Zhang^{1,*}, Alexander Karner^{1,*}, Kathrin Kostorz¹, Sophia Shea¹, David Steyrl¹, Filip
4 Melinscak¹, Ronald Sladky¹, Cindy Sumaly Lor^{1,†}, Frank Scharnowski^{1,†}

5 * These authors contributed equally to this work and share first authorship

6 † These authors share senior authorship

7 Affiliations

8 ¹Department of Cognition, Emotion, and Methods in Psychology, University of Vienna, Vienna,
9 Austria

10 corresponding author(s): Mengfan Zhang (mengfan.zhang@univie.ac.at)

11 Abstract

12 Neuroimaging has greatly improved our understanding of phobic mechanisms. To expand on
13 these advancements, we present data on the heterogeneity of neural patterns in spider
14 phobia combined with various psychological dimensions of spider phobia, using spider-
15 relevant stimuli of various intensities. Specifically, we have created a database in which 49
16 spider-fearful individuals viewed 225 spider-relevant images in the fMRI scanner and
17 performed behavioral avoidance tasks before and after the fMRI scan. For each participant,
18 the database consists of the neuroimaging part, which includes an anatomical scan, 5 passive-
19 viewing and 2 resting-state functional runs in both raw and pre-processed form along with
20 associated quality control reports. Additionally, a behavioral section includes self-report
21 questionnaires and avoidance tasks collected in pre- and post-sessions. The dataset is well
22 suited for investigating neural mechanisms of phobias, brain-behavior correlations, and also
23 contributes to the existing phobic neuroimaging datasets with spider-fearful samples.

Measurements	Anatomical and functional brain measurements, Online and in-person behavioral measurements.
Technology type(s)	Magnetic resonance imaging
Sample Characteristic-Organism	Homo sapiens

29
30 Key Words: fMRI, MRI, spider phobia, arachnophobia, behavior

31 32 Background & Summary

33 Specific phobias are the most common anxiety disorders and can cause high levels of distress
34 in affected individuals (e.g., Marks, 1987; Wardenaar et al., 2017). Spider phobia, which is
35 defined by intense and exaggerated fear of spiders (American Psychiatric Association, 2013),
36 is observed in a particularly large proportion of the population, with prevalence estimates
37 ranging from 2.7% up to 9.5% (Fredrikson et al., 1996; Oosterink et al., 2009; Zsido, 2017).
38 With the help of neuroimaging, researchers can gain insights into the neural underpinnings of
39 such specific phobias. Particularly functional magnetic resonance imaging (fMRI) has revealed
40 brain correlates of emotions and psychological dimensions relevant to spider phobia (for a
41 review, see Hinze et al., 2021). Neuroimaging studies have identified a so-called “fear

42 “network” in the processing of spider-related stimuli, which consists of the amygdala, the insula
43 and the anterior cingulate cortex (Hinze et al., 2021; Holzschneider & Mulert, 2011). Other
44 studies have suggested that disgust, which has been linked to the prevention of contamination
45 (e.g., Davey, 1994; Gerdes et al., 2009; Olatunji & McKay, 2006), is associated with overlapping
46 but distinct neural activation compared to fear (Stark et al., 2007). As negative emotions, both
47 fear and disgust are linked to avoidance behavior (e.g., Solarz, 1960), which is a key symptom
48 of anxiety disorders (American Psychiatric Association, 2013). While phobic individuals tend
49 to avoid the respective aversive stimulus, those who want to overcome their aversion may
50 choose to approach the stimulus to expose themselves, resulting in an approach-avoidance
51 conflict (Lewin, 1935). A variety of brain correlates of the approach-avoidance conflict have
52 been proposed and include the inferior frontal gyrus, as well as the right dorsolateral
53 prefrontal cortex (for details see Zorowitz et al., 2019). These findings can serve as a basis for
54 further investigation of the specific underlying neural patterns in spider phobic individuals
55 (Rosenbaum et al., 2020). Importantly, spider phobia is not a uniform condition (Knopf &
56 Pössel, 2009). Individuals with spider phobia may have different levels of fear, disgust,
57 avoidance behavior, and physiological responses (e.g., Schienle et al., 2005). This
58 heterogeneity can make it challenging to identify consistent neural patterns across individuals.
59 One goal of the current research is to address this heterogeneity issue by investigating
60 psychological dimensions relevant to spider phobia and their brain correlates.

61
62 Besides neuroimaging, it is important to investigate spider phobia at the behavioral level. First,
63 self-report questionnaires have been shown to indicate different levels of fear of spiders (e.g.,
64 Rinck et al., 2002), as well as related emotions and psychological constructs such as disgust, or
65 state- and trait-anxiety (e.g., Laux et al., 1981; Schienle et al., 2002, 2010). Second, behavioral
66 avoidance tests (BATs), in which spider-fearful individuals are asked to approach a spider, are
67 important measures that can provide further insight into avoidance behavior (e.g., Antony et
68 al., 2002; Muris et al., 1998). More recently, some computerized versions of BATs have been
69 developed (e.g., Grill et al., 2023; Mühlberger et al., 2008). Despite the availability of these
70 measures, knowledge of how behavioral data relate to brain data is limited. This knowledge
71 could greatly benefit clinical applications and the development of tailored interventions
72 (McNally, 2007).

73
74 Here, we present behavioral and MRI data of 49 individuals with fear of spiders. Specifically,
75 we collected behavioral data consisting of a variety of self-report questionnaires that are
76 highly relevant to fear of spiders, a physical behavioral avoidance test with a real spider, and
77 a novel computerized behavioral avoidance test. Moreover, participants underwent an
78 extensive MRI scan with a passive-viewing task, in which they were presented with images
79 depicting spiders and neutral images. A resting-state scan was performed both before and
80 after the passive-viewing task. Anatomical data were also acquired. After the MRI
81 appointment, participants rated the spider images they had been presented with on a 101-
82 point scale, according to “fear”, “disgust” and “willingness to approach”. Finally, participants
83 underwent two follow-up assessments to examine a potential reduction in fear of spiders. As
84 a result, the present study not only provides a large neuroimaging dataset, but also combines
85 a broad variety of measurements, including both conventional and novel approaches. A subset
86 of the data was analysized (but not released) in a previous study (Lor et al., 2023). Specifically,

87 we used resting-state data from 37 out of 49 participants to compare functional connectivity
88 before and after the passive-viewing task. We found decreased thalamo-cortical and increased
89 intra-thalamic connectivity, suggesting that resting-state measures can be affected by prior
90 emotion-inducing tasks and need to be carefully considered when detecting clinical
91 biomarkers. The remainder of the data has not been previously used and the dataset is suitable
92 for many questions investigating the neural mechanisms of phobias, fear processing,
93 correlation between brain activity and phobic behavior as well as appraisal, interventions, and
94 treatments, etc. This dataset also contributes to the growing collection of open MRI datasets,
95 in particular it contains neural responses from spider-fearful individuals that are relatively
96 difficult to access.

97

98 **Methods**

99 **Participants**

100 Fifty-one healthy, German-speaking individuals (41 female, 10 male) between the ages of 18
101 and 37 (mean = 22.65 ± 3.54) with self-reported fear of spiders and the willingness to
102 overcome their fear participated in the study. Due to technical reasons, two participants had
103 to be excluded from the dataset and the analysis, resulting in a total of 49 participants (40
104 female, 9 male; mean age = 22.55 ± 3.52 , min = 18, max = 37). Participants were recruited via
105 the university's participant database, where they received an invitation and indicated their
106 interest in participating. After signing up, they received an MRI safety questionnaire to
107 evaluate their suitability to undergo an MRI examination and filled out the German Spider Fear
108 Screening Questionnaire (SAS, Rinck et al., 2002; mean = 15.9 ± 4.4) where they had to score
109 a minimum of 8 out of 24 points, indicating at least a moderate fear of spiders. Other exclusion
110 criteria were self-reported past or current diagnosed psychiatric illnesses, pregnancy, or a
111 history of alcohol or drug abuse. Participants received a financial compensation of 50€, with
112 some receiving additional 5€ to compensate them for a pre-participation COVID-19 testing
113 when required by the guidelines at the time. Data were collected between September 2021
114 and January 2023. The study was conducted in accordance with the Declaration of Helsinki
115 and approved by the Ethics Committee of the University of Vienna (IRB numbers: 00584,
116 00657).

117

118 **Stimuli**

119 The stimulus set used in the present study consisted of 225 images depicting spiders or spider-
120 related content, and was a subset of the 313 images from a spider image database previously
121 established by our lab
122 (https://osf.io/vmuza/?view_only=93ff65b6629e4ae08174accfc6f3273b). These images were
123 rated according to the dimensions of "fear", "disgust", and "willingness to approach" by
124 individuals with self-reported fear of spiders in a previous study (Karner et al., 2024). To select
125 225 images from the 313 images that differed the most on these 3 psychological dimensions,
126 ratings first underwent a whitening transformation to account for the different scaling of the
127 ratings and their covariance using the "whitening" package in R (R Core Team, 2023). Then we
128 used the "maximin" package to make a space-filling design using 225 images under the
129 consideration of maximum-minimum distance. Some images depicted cobwebs, cartoon
130 spiders or small spiders, while other images showed large spiders such as tarantulas or
131 huntsman spiders, spiders eating prey, spiders in contact with human skin, or similar. All

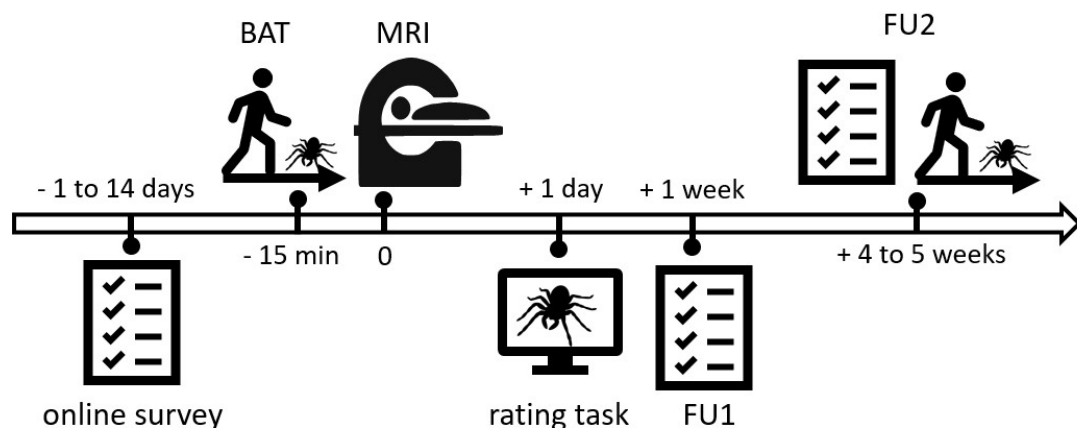
132 images had a size of 800×600 pixels and were upscaled to 1000×750 pixels for the passive-
133 viewing fMRI scan.

134

135 **Experimental Procedures**

136 The experiment consisted of a set of online surveys with self-report questionnaires, a
137 behavioral avoidance test (BAT) with an actual spider, a computerized BAT, a passive-viewing
138 MRI scan, ratings of spider images, as well as two follow-up sessions. An overview of the
139 experimental design is provided in Figure 1.

140



141

142 **Figure 1.** Overview of the experimental design. After confirming eligibility for participation in the study,
143 participants received a link to an online survey with self-report questionnaires, that was filled out
144 between 1 and 14 days prior to the MRI appointment. On the day of the MRI appointment, participants
145 underwent a behavioral avoidance test (BAT) with a spider, and a computerized BAT. Approximately 15
146 minutes after completing the BATs, they underwent an MRI scan, during which they were presented
147 with spider images on a screen. One day after the MRI appointment, participants received a link to an
148 online image rating task, in which they rated the images they had been presented with according to
149 "fear", "disgust", and "willingness to approach". One week after the MRI appointment, participants
150 engaged in a brief online follow-up (FU1), there they filled out a self-report questionnaire. Between 4
151 and 5 weeks after the MRI appointment, participants underwent a second follow up (FU2), which
152 consisted of a self-report questionnaire, a BAT, and a computerized BAT.

153

154 **Self-Report Questionnaires**

155 At a time point between one and 14 days prior to the MRI appointment, participants received
156 a link to an online questionnaire on the SoSci platform of University of Vienna (Leiner, 2019),
157 where they answered self-report questionnaires indicating their level of fear of spiders,
158 specifically the German validated versions of the Fear of Spiders Questionnaire (FSQ;
159 Szymanski & O'Donohue, 1995) and the Spider Phobia Questionnaire (Watts & Sharrock,
160 1984), that were introduced by Rinck et al. (2022), together with the German Spider
161 Screening (Rinck et al., 2002). Additionally, participants filled out questionnaires indicating
162 state- and trait anxiety (STAI; Laux et al., 1981), disgust propensity (FEE; Schienle et al., 2002)
163 and disgust sensitivity (SEE; Schienle et al., 2010). Demographic information was also
164 collected.

165

166 **Behavioral Avoidance Test**

167 On the day of the MRI appointment, participants came to the University of Vienna, where they
168 underwent a BAT, in which they were asked to approach a terrarium containing a spider. The
169 spider was a real huntsman spider (*Heteropoda* ssp.; Latreille, 1804), which was inanimate and
170 prepared in a natural-looking position. Participants were unaware that the spider was not
171 alive. Before entering the room with the terrarium, they received the following instructions
172 from the experimenter: *"In this room, we have a terrarium containing a spider. We would like*
173 *to ask you to approach the terrarium up until a point where you still feel comfortable, and then*
174 *stop and let us know. If you want to go all the way to the terrarium and feel comfortable, you*
175 *may open the transparent lid, but you don't have to do this."* (translated from German) Then,
176 the experimenter opened the door to the room with the terrarium and asked the participants
177 to position their right foot behind a cross on the floor, which was 4.5 meters away from the
178 terrarium. The experimenter remained standing in the door frame. While participants
179 approached the terrarium, the distance covered was measured in centimetres using a laser
180 distance meter that was always positioned in the same predefined spot and directed towards
181 the participant's leg. Specifically, we measured the start and end distance, to calculate the net
182 distance that participants walked towards the terrarium. Two different terrariums (terrarium
183 A and terrarium B) with identical spiders, but slightly different interior was used within the
184 scope of the study to prevent potential biases due to static mental representations of the
185 terrarium. Half of the participants approached terrarium A on the day of the MRI appointment
186 and terrarium B on the day of the follow-up appointment, and vice versa.

187

188 **Computerized Behavioral Avoidance Test**

189 In addition to the BAT, participants underwent a novel computerized BAT that was designed
190 based on the work of (Peirce et al., 2019) and implemented in PsychoPy. In this task,
191 participants needed to sharpen three highly blurred images of spiders up until a point where
192 they still felt comfortable looking at them by dragging a slider on the screen. Although the
193 scale was linear, with values from 1 to 101 stored, the sharpening of the images occurred in a
194 logarithmic manner. The experiment was set up in PsychoPy and adapted from the script of
195 Peirce et al. (2019). At the start of the computerized BAT, participants read the following
196 instructions on the screen: *"On the following pages, you will see blurred, unrecognizable*
197 *images of spiders. Use the slider to sharpen each image to the point where you still feel*
198 *comfortable looking at it. Important: Keep the left mouse button pressed while moving the*
199 *slider. As soon as you release the left mouse button, your answer will be saved. We will start*
200 *with a practice round with a neutral image. This will be followed by the spider images. If you*
201 *want to start, press the Space key."* (translated from German) The practice image consisted of
202 a chair on a wooden floor, followed by three spider images displaying large and hairy spiders.
203 Contrary to the BAT, the experimenter left the room while participants engaged in the
204 computerized BAT. During 11 computerized BATs (6 before the MRI appointment, 5 at follow-
205 up 2) the experimenter remained present in the room with the participant. The order of
206 performing the BAT first or the computerized BAT first was counterbalanced.

207

208 **Passive-Viewing MRI Scan**

209 After completing the BAT and computerized BAT, participants underwent a brain scan at the
210 University of Vienna's MR Center. To reduce head motion, easily removable, non-constrictive
211 piece of tape was placed on the participant's forehead to provide tactile feedback as described

212 by (Krause et al., 2019). Stimuli were presented to participants on an MR-compatible LCD
213 screen (BOLDscreen 32 LCD for fMRI, Cambridge Research Systems) that was positioned at the
214 head of the scanner bore. Participants were able to view the screen through a mirror mounted
215 onto the head coil. First, a resting-state scan was performed during which participants were
216 instructed to relax and keep their eyes open and directed at a fixation point. Subsequently,
217 participants engaged in a passive-viewing task that consisted of five runs. In each run,
218 participants were presented with 45 spider images, which displayed spiders and spider-related
219 content, as well as with 15 neutral images depicting inanimate objects. Each image
220 presentation lasted for 4 seconds and was followed by a presentation of the fixation point for
221 2-3 seconds. All images had a size of 1000×750 pixels. In each run, participants also underwent
222 6 catch trials, in which they were instructed to press a specific button on a button box that
223 was positioned in their hand (e.g. *“Please press the left button now.”*). Once a catch trial was
224 completed, the next image was presented to the participant. As an additional attention check,
225 the experimenters used the live video of an eye tracker to see whether participants were
226 keeping their eyes open, which was communicated to the participants beforehand. After runs
227 1, 3 and 5, participants were asked about their current levels of agitation and exhaustion,
228 which they stated via the intercom on a scale from 0 to 10. The five passive-viewing runs were
229 followed by another resting-state scan which was identical to the first resting-state scan. This
230 was followed by a structural scan, which marked the end of the scanning session. The MRI
231 data therefore consist of 7 functional runs, 5 passive viewing runs and two resting state runs,
232 as well as a structural scan.

233

234 ***Image Ratings***

235 One day after the MRI appointment, participants received an email with links to the University
236 of Vienna's SoSci (Leiner, 2019) platform, where they were asked to rate all spider images that
237 had been presented to them during the passive viewing fMRI scan. The ratings were
238 administered in three blocks (A, B. and C), each consisting of 75 images. The images were
239 presented in their original size of 800x600 pixels. Participants were allowed to take breaks
240 between the blocks, with the requirement to complete all three blocks within 48 hours after
241 receiving the links. However, ratings that were administered within one week after the fMRI
242 appointment were also accepted by the research team. The image rating procedure was as
243 follows: Each block started with a practice round, followed by the actual image ratings. In each
244 image rating trial, an image was presented on the screen for 3 seconds. Then the image
245 disappeared, and 3 questions and corresponding rating scales were presented on the screen.
246 (1) “How much fear does this picture elicit in you?”; (2) “How much disgust does this picture
247 elicit in you?”; (3) “How close could you come to the content shown in the picture, if you
248 wanted to overcome your aversion?” (translated from German). Ratings were made by moving
249 a continuously adjustable slider on a 101-point visual analog scale. In each trial, participants
250 were given 12 seconds to administer the three ratings. To proceed with the next image, they
251 clicked “Next” in the bottom-right corner on the screen. Each block contained a break
252 questionnaire, in which participants stated their current levels of fear, physical arousal,
253 disgust, boredom and exhaustion in subjective units of distress (Wolpe, 1969) on a scale from
254 0-10. Additionally, each break questionnaire contained a bogus item to test the participants'
255 attention (e.g., Meade & Craig, 2012).

256

257 ***Follow-up Assessments***

258 One week after the MRI appointment, participants received a link to an online questionnaire
259 where they were asked to fill out the FSQ a second time (follow-up 1). A total of 38 out of 49
260 participants completed follow-up 1. Follow-up 2 took place between 4 and 5 weeks after the
261 MRI appointment. Participants returned to the University of Vienna, where they first filled out
262 the FSQ a third time and then underwent the BAT and computerized BAT for a second time.
263 Thirteen participants filled out the FSQ after having completed the BAT and computerized BAT.
264 Participants were then asked to fill out a brief feedback sheet asking them about their
265 thoughts on the study, and whether they noticed anything special. A total of 46 out of 49
266 participants completed follow-up 2. Out of all the participants, only one person expressed
267 doubt about the authenticity of the spider. The feedback sheet marked the end of the
268 participation in the experiment.

269

270 ***MRI Acquisition***

271 All functional and structural scans were collected using a 3T Siemens MAGNETOM Skyra MRI
272 scanner (Siemens, Erlangen, Germany) with a 32-channel head coil, located at the University
273 of Vienna. Functional data were acquired with an interleaved mode, using a T2*-weighted
274 echo planar imaging sequence with multiband acceleration factor 4, TR = 1250 ms, TE = 36 ms,
275 voxel size = 2 mm * 2mm * 2mm, flip angle = 65 degrees, field of view (FOV) = 192 mm * 192
276 mm * 145 mm, 56 slices without slice gap to cover the full brain, and anterior-posterior phase
277 encoding. The total scan duration for each resting state run was 9:00 mins, and 7:20 mins for
278 each passive viewing run. After the functional runs, a field map was collected with a short echo
279 time of 4.92 ms and a long echo time of 7.38 ms.
280 Structural data for each participant was acquired using a single-shot, high-resolution MPRAGE
281 sequence with an acceleration factor of 2 using GRAPPA with TR = 2300 ms, TE = 2.43 ms, voxel
282 size = 0.8 mm * 0.8 mm * 0.8 mm, flip angle = 8 degrees, and field of view (FOV) = 263 mm *
283 350 mm * 350 mm. The total duration of the structural data acquisition was 6:35 mins.

284

285 ***MRI Preprocessing***

286 The pre-processed data included in this dataset was performed with fMRIprep 20.2.6 (Esteban
287 et al., 2019), which is based on Nipype 1.7.0 (Gorgolewski et al., 2011).

288

289 ***Anatomical data preprocessing***

290 The T1-weighted (T1w) images were first corrected for intensity non-uniformity (INU) using
291 N4BiasFieldCorrection (Tustison et al., 2010), and used as T1w-reference throughout the
292 workflow. Then, the T1w-reference was skull-stripped with antsBrainExtraction.sh workflow,
293 using OASIS30ANTS as the target template. Brain tissue segmentation of cerebrospinal fluid
294 (CSF), white-matter (WM) and gray-matter (GM) was performed on the brain-extracted T1w
295 using the software fast (FSL 5.0.9, RRID:SCR_002823, Zhang et al., 2001). Volume-based spatial
296 normalization to the standard space (MNI152NLin2009cAsym) was performed through
297 nonlinear registration using antsRegistration (ANTS 2.3.3), with brain-extracted versions of
298 both T1w reference and T1w template.

299

300 ***Functional data preprocessing***

301 For each of the 7 functional runs per subject, the following procedures were performed: First,
302 a reference volume and its skull-stripped version were generated using a custom methodology
303 of fMRIprep. A B_0 -nonuniformity map (i.e. fieldmap) was estimated based on a phase-
304 difference map calculated with a dual-echo GRE (gradient-recall echo) sequence, processed
305 with a custom workflow of SDCFlows. The field map was then co-registered to the target EPI
306 (echo-planar imaging) reference run and converted to a displacement field map with FSL's
307 fugue and other SDCflows tools. Based on the estimated susceptibility distortion, a corrected
308 EPI reference was calculated for a more accurate co-registration with the anatomical
309 reference. The reference was then co-registered to the T1w reference using flirt, and the co-
310 registration was configured with nine degrees of freedom to account for distortions remaining
311 in the reference. Head-motion parameters (transformation matrices, and six corresponding
312 rotation and translation parameters) were estimated before any spatiotemporal filtering using
313 mcflirt (Jenkinson et al., 2002). BOLD runs were slice-time corrected to 0.571s using 3dTshift
314 (Cox & Hyde, 1997). The fMRI time-series were resampled onto their original, native space by
315 applying a single, composite transform to correct for head-motion and susceptibility
316 distortions. Also, the fMRI time-series were resampled into standard space, generating a
317 preprocessed functional run in the MNI152NLin2009cAsym space. Several confounding time-
318 series were calculated based on the preprocessed BOLD: framewise displacement (FD), DVARS
319 and three region-wise global signals. FD and DVARS were calculated for each functional run,
320 both using their implementations in Nipype, and the three global signals were extracted within
321 the CSF, the WM and the whole-brain masks. Additionally, a set of physiological regressors
322 were extracted to allow for component-based noise correction (CompCor, Behzadi et al.,
323 2007). Principal components were estimated after high-pass filtering the preprocessed fMRI
324 time-series for the two CompCor variants: temporal (tCompCor) and anatomical (aCompCor).
325 tCompCor components were then calculated from the top 2% variable voxels within the brain
326 mask. For aCompCor, three probabilistic masks (CSF, WM and combined CSF+WM) were
327 generated in anatomical space. From these masks, a mask of voxels likely to contain a volume
328 fraction of GM was subtracted and then resampled in BOLD space. The head-motion estimates
329 calculated in the correction step were also placed within the corresponding confounds files.
330 All resamplings were performed with a single interpolation step by composing all the pertinent
331 transformations. (i.e. head-motion transform matrices, susceptibility distortion correction
332 when available, and co-registrations to anatomical and output spaces). Gridded (volumetric)
333 resamplings were performed using antsApplyTransforms (ANTs), configured with Lanczos
334 interpolation to minimize the smoothing effects of other kernels (Lanczos, 1964). Non-gridded
335 (surface) resamplings were performed using mri_vol2surf (FreeSurfer).
336

337 Many internal operations of fMRIprep use Nilearn 0.6.2 (Abraham et al., 2014;
338 RRID:SCR_001362), mostly within the functional processing workflow. For more details of the
339 pipeline, see the section corresponding to workflows in fMRIprep's documentation
340 (<https://fmriprep.org/en/20.2.6/workflows.html>).

341

342 **Data Records**

343 The MRI dataset is organized according to the Brain Imaging Data Structure (BIDS; Gorgolewski
344 et al., 2016) specification (version 1.0.1) and evaluated with the MRI Quality Control tool
345 (MRIQC) version 1.4.0 (Esteban et al., 2017). All imaging data, including preprocessed data

346 with fMRIprep version 20.2.6 (under the "derivatives/fmriprep" directory) and quality
347 assessment reports with MRIQC version 1.4.0 (under the "derivative/mriqc" directory) are
348 available on OpenNeuro (<https://openneuro.org/datasets/ds004630>). The behavioural data,
349 the corresponding codebooks and the computerized BAT are available on OSF
350 (<https://osf.io/w4s2h/>). We set up a GitHub repository
351 (<https://github.com/univiemops/spider20-fmri-data>) to share the data descriptions and the
352 preprocessing and analysis scripts.

353

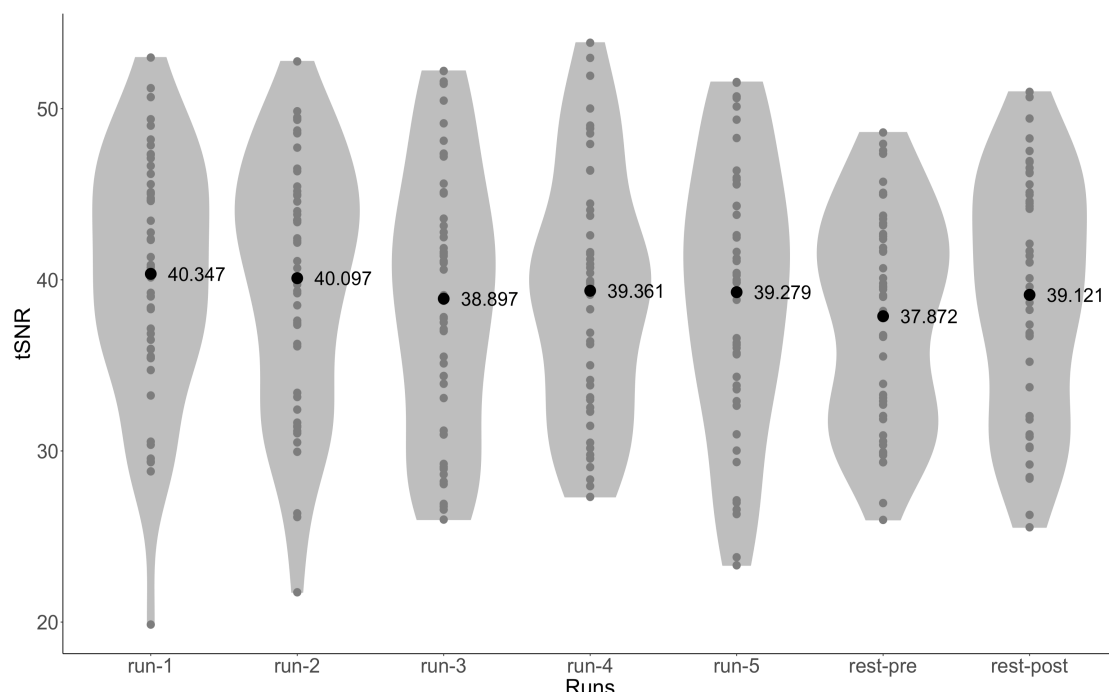
354 **Technical Validation**

355 **Quality Assessment**

356 To assess the quality of the current dataset, we used an open-source BIDS application, MRIQC,
357 to automatically generate Image Quality Metrics (IQMs) and visual quality reports for
358 individual and group levels. Individual functional reports were generated per subject per run
359 to show the mosaic view of the average BOLD signal map, standard deviation from average
360 BOLD signal map, summary plot of motion-related indices, and IQMs. The IQMs include
361 commonly used measures of spatial and temporal signal quality (e.g., signal-to-noise ratio
362 (SNR), temporal SNR (tSNR, Figure 2), DVARS) and measures of artifacts (e.g., framewise
363 displacement (FD, Figure 3), number of dummy scans). The individual anatomical reports
364 include a mosaic zoomed-in brain mask map, a background noise map, IQMs including noise
365 measurements. The group functional and anatomical reports visualize the IQMs across
366 participants by displaying a box plot per measure. These reports graphically show the range
367 and outliers of quality measures and can be used to quickly compare participants. All reports
368 and accompanying JSON and TSV files are shared on OpenNeuro.

369

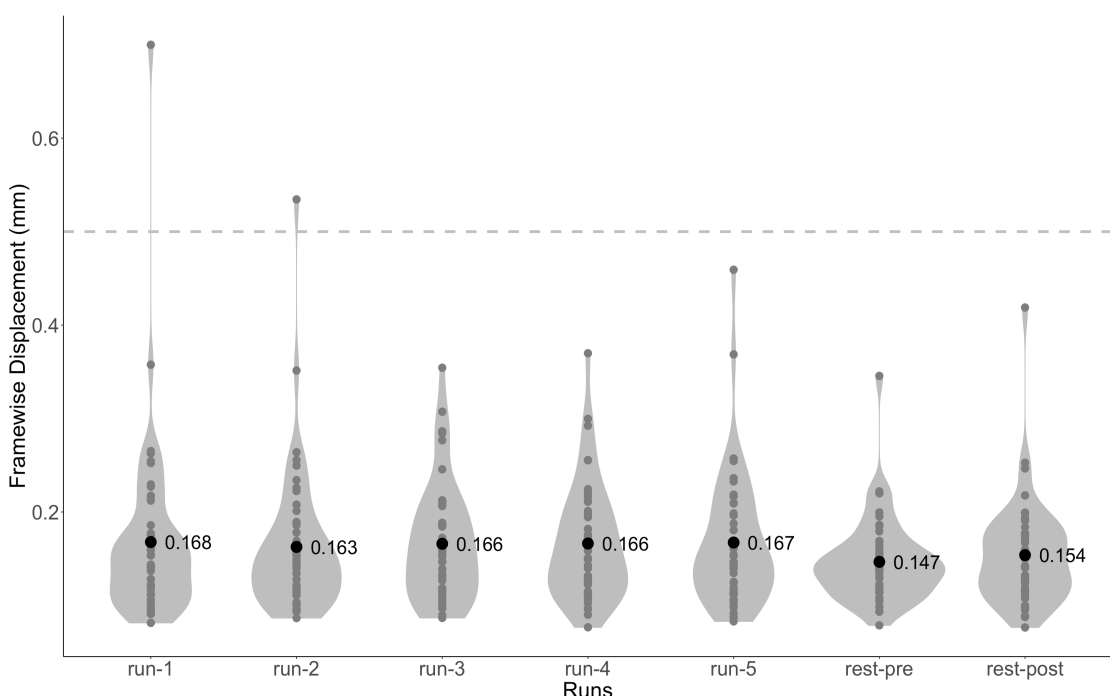
370



371

372 **Figure 2.** Temporal SNR of each run across all participants. Gray dots represent the individual tSNR for
373 that run. Black dots and associated values are the mean tSNR across all participants for that run. The
374 mean whole-brain tSNR across participants for all runs was 39.28 ± 7.20 .

375



376

377

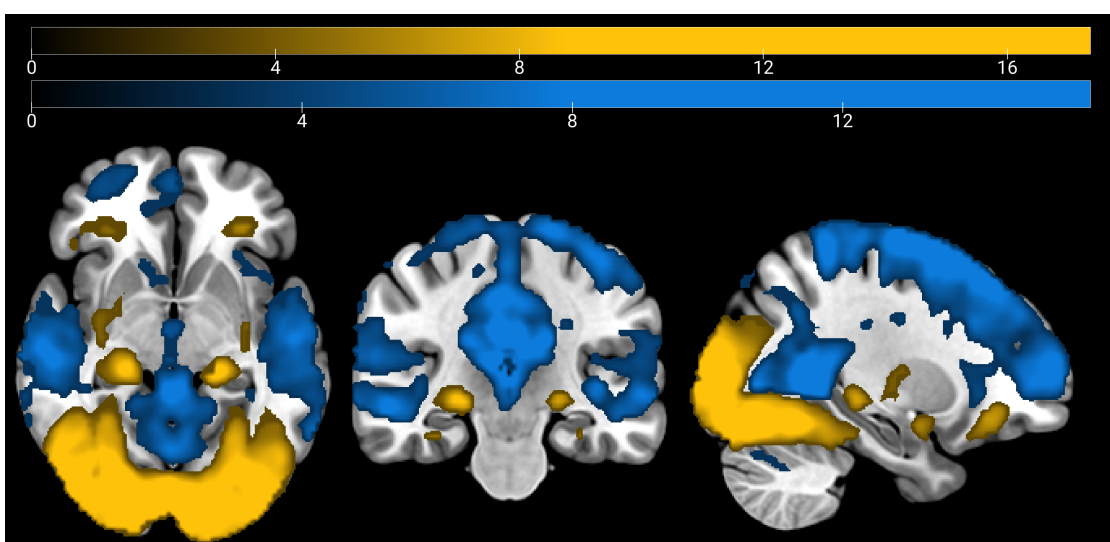
378 **Figure 3.** Framewise displacement of each run across all participants. Gray dots represent the individual
379 FD for that run. Black dots and associated values are the mean FD across all participants for that run.
380 Participant movement is low in this dataset, only 2 runs of one participant had higher than 0.5mm FD.
381 The mean FD across participants for all runs was 0.16 ± 0.07 mm.

382

383 **Basic analysis of stimuli vs. implicit baseline**

384 To further validate the dataset, we performed a basic general linear model (GLM) analysis to
385 show brain activation during stimulus presentation compared to an implicit baseline. This
386 analysis should find positive voxel activation in visual areas and task-related regions, such as
387 the hippocampus and the amygdala. For this purpose, we used the fMRIprep-preprocessed
388 passive-viewing functional scans and Statistical Parametric Mapping (SPM12; Wellcome Trust
389 Centre for Neuroimaging, London, United Kingdom) for the GLM analysis. Runs for which the
390 maximum framewise displacement (FD) exceeded 5mm were excluded from the analysis (2
391 runs of one participant). For the first-level analysis, we specified two regressors, one for the
392 onsets of stimulus presentation (including spider images and neutral images) and one for the
393 onsets of the button-press catch trials. Each stimulus was modelled as a boxcar function, with
394 lengths matching each stimulus duration, and convolved with the hemodynamic response
395 function. The six motion realignment parameters were added as nuisance regressors. We
396 performed a one-sample t-test second-level analysis, one for positive activation and one for
397 negative activation, using the first-level activation maps that correspond to the "stimuli"
398 regressor from the 49 participants. We applied a family-wise error corrected cluster threshold
399 of $p < 0.05$, with height threshold set at $p < 0.001$. As expected, we found positive activation in
400 visual areas, as well as fear-related regions such as the bilateral amygdala, hippocampus and
401 putamen. Conversely, we found negative activation in regions associated with resting-state
402 such as parts of the default-mode network among other regions. This outcome is consistent
403 with the previous literature on similar experimental paradigms (Botvinik-Nezer et al., 2019).

403



404

405

406

407

Figure 4. Brain activation clusters for stimulus presentation vs. implicit baseline ($p<0.001$ for peak threshold and $p<0.05$ for FWE-cluster correction). Blue: negative activation; yellow: positive activation. N=49.

408

Code Availability

409

410

411

412

All code is available in the GitHub repository (<https://github.com/univiemops/spider20-fmri-data>). The code includes scripts for experiment presentation (executed in Python and largely relied on PsychoPy (Peirce, 2007)), data sorting, preprocessing and quality control (executed in shell scripting), and analyses (executed in Matlab).

413

414

Acknowledgements

415

416

417

418

419

FM was funded by the Austrian Science Fund (FWF) [10.55776/ESP133]. KK was funded by the Austrian Science Fund (FWF) [10.55776/ESP286]. FS was supported by the Swiss National Science Foundation (BSSG10_155915, 100014_178841, 32003B_166566), the Foundation for Research in Science and the Humanities at the University of Zurich (STWF-17-012), and the Baugarten Stiftung.

420

421

Author contributions

422

423

424

425

426

427

428

429

430

MZ: Conceptualization, Formal Analysis, Investigation, Data Curation, Validation, Visualization, Writing - Original Draft. AK: Conceptualization, Methodology, Software, Formal Analysis, Investigation, Data Curation, Writing - Original Draft. KK: Conceptualization, Data Curation, Writing - Review & Editing. SS: Investigation, Writing - Review & Editing. DS: Conceptualization, Writing - Review & Editing. RS: Methodology, Resources, Writing - Review & Editing. FM: Software, Writing - Review & Editing. CL: Conceptualization, Methodology, Software, Validation, Formal Analysis, Investigation, Data Curation, Writing - Original Draft. FS: Conceptualization, Project Administration, Methodology, Supervision, Funding Acquisition, Resources, Writing - Review & Editing.

431

432

Competing interests

433

The authors declare no competing interests.

434 **References**

- 435 1. Abraham, A., Pedregosa, F., Eickenberg, M., Gervais, P., Mueller, A., Kossaifi, J.,
436 Gramfort, A., Thirion, B., & Varoquaux, G. (2014). Machine learning for neuroimaging
437 with scikit-learn. *Frontiers in Neuroinformatics*, 8, 14.
438 <https://doi.org/10.3389/fninf.2014.00014>
- 439 2. American Psychiatric Association. (2013). *Diagnostic and statistical manual of mental*
440 *disorders: DSM-5TM, 5th ed* (pp. xliv, 947). American Psychiatric Publishing, Inc.
441 <https://doi.org/10.1176/appi.books.9780890425596>
- 442 3. Behzadi, Y., Restom, K., Liau, J., & Liu, T. T. (2007). A component based noise correction
443 method (CompCor) for BOLD and perfusion based fMRI. *NeuroImage*, 37(1), 90–101.
444 <https://doi.org/10.1016/j.neuroimage.2007.04.042>
- 445 4. Botvinik-Nezer, R., Iwanir, R., Holzmeister, F., Huber, J., Johannesson, M., Kirchler, M.,
446 Dreber, A., Camerer, C. F., Poldrack, R. A., & Schonberg, T. (2019). fMRI data of mixed
447 gambles from the Neuroimaging Analysis Replication and Prediction Study. *Scientific*
448 *Data*, 6(1), Article 1. <https://doi.org/10.1038/s41597-019-0113-7>
- 449 5. Cox, R. W., & Hyde, J. S. (1997). Software tools for analysis and visualization of fMRI
450 data. *NMR in Biomedicine*, 10(4–5), 171–178. [https://doi.org/10.1002/\(SICI\)1099-1492\(199706/08\)10:4/5<171::AID-NBM453>3.0.CO;2-L](https://doi.org/10.1002/(SICI)1099-1492(199706/08)10:4/5<171::AID-NBM453>3.0.CO;2-L)
- 452 6. Davey, G. C. L. (1994). The “Disgusting” Spider: The Role of Disease and Illness in the
453 Perpetuation of Fear of Spiders. *Society & Animals*, 2(1), 17–25.
454 <https://doi.org/10.1163/156853094X00045>
- 455 7. Esteban, O., Birman, D., Schaer, M., Koyejo, O. O., Poldrack, R. A., & Gorgolewski, K. J.
456 (2017). MRIQC: Advancing the automatic prediction of image quality in MRI from
457 unseen sites. *PLOS ONE*, 12(9), e0184661.
458 <https://doi.org/10.1371/journal.pone.0184661>
- 459 8. Esteban, O., Markiewicz, C. J., Blair, R. W., Moodie, C. A., Isik, A. I., Erramuzpe, A., Kent,
460 J. D., Goncalves, M., DuPre, E., Snyder, M., Oya, H., Ghosh, S. S., Wright, J., Durnez, J.,
461 Poldrack, R. A., & Gorgolewski, K. J. (2019). fMRIprep: A robust preprocessing pipeline
462 for functional MRI. *Nature Methods*, 16(1), Article 1. <https://doi.org/10.1038/s41592-018-0235-4>
- 464 9. Fredrikson, M., Annas, P., Fischer, H., & Wik, G. (1996). Gender and age differences in
465 the prevalence of specific fears and phobias. *Behaviour Research and Therapy*, 34(1),
466 33–39. [https://doi.org/10.1016/0005-7967\(95\)00048-3](https://doi.org/10.1016/0005-7967(95)00048-3)
- 467 10. Gerdes, A. B. M., Uhl, G., & Alpers, G. W. (2009). Spiders are special: Fear and disgust
468 evoked by pictures of arthropods. *Evolution and Human Behavior*, 30(1), 66–73.
469 <https://doi.org/10.1016/j.evolhumbehav.2008.08.005>
- 470 11. Gorgolewski, K., Burns, C., Madison, C., Clark, D., Halchenko, Y., Waskom, M., & Ghosh,
471 S. (2011). Nipype: A Flexible, Lightweight and Extensible Neuroimaging Data
472 Processing Framework in Python. *Frontiers in Neuroinformatics*, 5.
473 <https://www.frontiersin.org/article/10.3389/fninf.2011.00013>
- 474 12. Gorgolewski, K. J., Auer, T., Calhoun, V. D., Craddock, R. C., Das, S., Duff, E. P., Flandin,
475 G., Ghosh, S. S., Glatard, T., Halchenko, Y. O., Handwerker, D. A., Hanke, M., Keator,
476 D., Li, X., Michael, Z., Maumet, C., Nichols, B. N., Nichols, T. E., Pellman, J., ... Poldrack,
477 R. A. (2016). The brain imaging data structure, a format for organizing and describing

478 outputs of neuroimaging experiments. *Scientific Data*, 3(1), Article 1.
479 <https://doi.org/10.1038/sdata.2016.44>

480 13. Grill, M., Heller, M., & Haberkamp, A. (2023). *Development and validation of an open-*
481 *access online Behavioral Avoidance Test (BAT) for spider fear*.
482 <https://doi.org/10.31234/osf.io/5k497>

483 14. Hinze, J., Röder, A., Menzie, N., Müller, U., Domschke, K., Riemenschneider, M., & Noll-
484 Hussong, M. (2021). Spider Phobia: Neural Networks Informing Diagnosis and
485 (Virtual/Augmented Reality-Based) Cognitive Behavioral Psychotherapy-A Narrative
486 Review. *Frontiers in Psychiatry*, 12, 704174.
487 <https://doi.org/10.3389/fpsyg.2021.704174>

488 15. Holzschneider, K., & Mulert, C. (2011). Neuroimaging in anxiety disorders. *Dialogues*
489 *in Clinical Neuroscience*, 13(4), 453–461.
490 <https://www.ncbi.nlm.nih.gov/pmc/articles/PMC3263392/>

491 16. Jenkinson, M., Bannister, P., Brady, M., & Smith, S. (2002). Improved Optimization for
492 the Robust and Accurate Linear Registration and Motion Correction of Brain Images.
493 *NeuroImage*, 17(2), 825–841. <https://doi.org/10.1006/nimg.2002.1132>

494 17. Karner, A., Zhang, M., Lor, C. S., Steyrl, D., Götzendorfer, S., Weidt, S., Melinscak, F., &
495 Scharnowski, F. (2024). The "SpiDa" dataset: Self-report questionnaires
496 and ratings of spider images from spider-fearful individuals. *Frontiers in Psychology*,
497 15. <https://doi.org/10.3389/fpsyg.2024.1327367>

498 18. Knopf, K., & Pössel, P. (2009). Individual response differences in spider phobia:
499 Comparing phobic and non-phobic women of different reactivity levels. *Anxiety,*
500 *Stress, and Coping*, 22(1), 39–55. <https://doi.org/10.1080/10615800802169358>

501 19. Krause, F., Benjamins, C., Eck, J., Lührs, M., van Hoof, R., & Goebel, R. (2019). Active
502 head motion reduction in magnetic resonance imaging using tactile feedback. *Human*
503 *Brain Mapping*, 40(14), 4026–4037. <https://doi.org/10.1002/hbm.24683>

504 20. Lanczos, C. (1964). A Precision Approximation of the Gamma Function. *Journal of the*
505 *Society for Industrial and Applied Mathematics Series B Numerical Analysis*, 1(1), 86–
506 96. <https://doi.org/10.1137/0701008>

507 21. Laux, L., Glanzmann, P. G., Schaffner, P., & Spielberger, C. D. (1981). *Das State-Trait-*
508 *Angstinventar STA*; *theoretische Grundlagen und Handanweisung*. Beltz Test.

509 22. Leiner, D. J. (2019). *SoSci survey (version 3.1. 06)[computer software]*.
510 <https://scholar.google.com/scholar?cluster=4857768626174197430&hl=en&oi=scholar>

511 23. Lewin, K. (1935). *A dynamic theory of personality* (pp. ix, 286). McGraw-Hill.

512 24. Lor, C. S., Zhang, M., Karner, A., Steyrl, D., Sladky, R., Scharnowski, F., & Haugg, A.
513 (2023). Pre- and post-task resting-state differs in clinical populations. *NeuroImage:*
514 *Clinical*, 37, 103345. <https://doi.org/10.1016/j.jneurol.2023.103345>

515 25. Marks, I. M. (1987). *Fears, Phobias, and Rituals: Panic, Anxiety, and Their Disorders*.
516 Oxford University Press.

517 26. McNally, R. J. (2007). Mechanisms of exposure therapy: How neuroscience can
518 improve psychological treatments for anxiety disorders. *Clinical Psychology Review*,
519 27(6), 750–759. <https://doi.org/10.1016/j.cpr.2007.01.003>

520 27. Meade, A. W., & Craig, S. B. (2012). Identifying careless responses in survey data.
521 *Psychological Methods*, 17(3), 437–455. <https://doi.org/10.1037/a0028085>

523 28. Mühlberger, A., Neumann, R., Wieser, M. J., & Pauli, P. (2008). The impact of changes
524 in spatial distance on emotional responses. *Emotion (Washington, D.C.)*, 8(2), 192–
525 198. <https://doi.org/10.1037/1528-3542.8.2.192>

526 29. Olatunji, B. O., & McKay, D. (2006). Further exploration of the role of disgust sensitivity
527 in anxiety and related disorders. *Anxiety, Stress & Coping*, 19(4), 331–334.
528 https://www.academia.edu/24853657/Further_exploration_of_the_role_of_disgust_sensitivity_in_anxiety_and_related_disorders

530 30. Oosterink, F. M. D., De Jongh, A., & Hoogstraten, J. (2009). Prevalence of dental fear
531 and phobia relative to other fear and phobia subtypes. *European Journal of Oral
532 Sciences*, 117(2), 135–143. <https://doi.org/10.1111/j.1600-0722.2008.00602.x>

533 31. Peirce, J., Gray, J. R., Simpson, S., MacAskill, M., Höchenberger, R., Sogo, H., Kastman,
534 E., & Lindeløv, J. K. (2019). PsychoPy2: Experiments in behavior made easy. *Behavior
535 Research Methods*, 51(1), 195–203. <https://doi.org/10.3758/s13428-018-01193-y>

536 32. Peirce, J. W. (2007). PsychoPy—Psychophysics software in Python. *Journal of
537 Neuroscience Methods*, 162(1), 8–13.
538 <https://doi.org/10.1016/j.jneumeth.2006.11.017>

539 33. R Core Team. (2023). *R: A Language and Environment for Statistical Computing* [R]. R
540 Foundation for Statistical Computing. <https://www.R-project.org/>

541 34. Rinck, M., Bundschuh, S., Engler, S., Müller, A., Wissmann, J., Ellwart, T., & Becker, E.
542 S. (2002). Reliabilität und Validität dreier Instrumente zur Messung von Angst vor
543 Spinnen. *Diagnostica*, 48(3), 141–149. <https://doi.org/10.1026/0012-1924.48.3.141>

544 35. Rosenbaum, D., Leehr, E. J., Krocze, A., Rubel, J. A., Int-Veen, I., Deutsch, K., Maier,
545 M. J., Hudak, J., Fallgatter, A. J., & Ehlis, A.-C. (2020). Neuronal correlates of spider
546 phobia in a combined fNIRS-EEG study. *Scientific Reports*, 10(1), Article 1.
547 <https://doi.org/10.1038/s41598-020-69127-3>

548 36. Schienle, A., Dietmaier, G., Ille, R., & Leutgeb, V. (2010). Eine Skala zur Erfassung der
549 Ekelsensitivität (SEE). *Zeitschrift Für Klinische Psychologie Und Psychotherapie*, 39(2),
550 80–86. <https://doi.org/10.1026/1616-3443/a000016>

551 37. Schienle, A., Schäfer, A., Walter, B., Stark, R., & Vaitl, D. (2005). Brain activation of
552 spider phobics towards disorder-relevant, generally disgust- and fear-inducing
553 pictures. *Neuroscience Letters*, 388(1), 1–6.
554 <https://doi.org/10.1016/j.neulet.2005.06.025>

555 38. Schienle, A., Walter, B., Stark, R., & Vaitl, D. (2002). Ein Fragebogen zur Erfassung der
556 Ekelempfindlichkeit (FEE). *Zeitschrift für Klinische Psychologie und Psychotherapie*,
557 31(2), 110–120. <https://doi.org/10.1026/0084-5345.31.2.110>

558 39. Solarz, A. K. (1960). Latency of instrumental responses as a function of compatibility
559 with the meaning of eliciting verbal signs. *Journal of Experimental Psychology*, 59,
560 239–245. <https://doi.org/10.1037/h0047274>

561 40. Stark, R., Zimmermann, M., Kagerer, S., Schienle, A., Walter, B., Weygandt, M., & Vaitl,
562 D. (2007). Hemodynamic brain correlates of disgust and fear ratings. *NeuroImage*,
563 37(2), 663–673. <https://doi.org/10.1016/j.neuroimage.2007.05.005>

564 41. Szymanski, J., & O'Donohue, W. (1995). Fear of Spiders Questionnaire. *Journal of
565 Behavior Therapy and Experimental Psychiatry*, 26(1), 31–34.
566 [https://doi.org/10.1016/0005-7916\(94\)00072-T](https://doi.org/10.1016/0005-7916(94)00072-T)

567 42. Tustison, N. J., Avants, B. B., Cook, P. A., Zheng, Y., Egan, A., Yushkevich, P. A., & Gee,
568 J. C. (2010). N4ITK: Improved N3 Bias Correction. *IEEE Transactions on Medical*
569 *Imaging*, 29(6), 1310–1320. <https://doi.org/10.1109/TMI.2010.2046908>

570 43. Wardenaar, K. J., Lim, C. C. W., Al-Hamzawi, A. O., Alonso, J., Andrade, L. H., Benjet,
571 C., Bunting, B., de Girolamo, G., Demyttenaere, K., Florescu, S. E., Gureje, O., Hisateru,
572 T., Hu, C., Huang, Y., Karam, E., Kiejna, A., Lepine, J. P., Navarro-Mateu, F., Oakley
573 Browne, M., ... de Jonge, P. (2017). The cross-national epidemiology of specific phobia
574 in the World Mental Health Surveys. *Psychological Medicine*, 47(10), 1744–1760.
575 <https://doi.org/10.1017/S0033291717000174>

576 44. Watts, F. N., & Sharrock, R. (1984). Questionnaire dimensions of spider phobia.
577 *Behaviour Research and Therapy*, 22(5), 575–580. [https://doi.org/10.1016/0005-7967\(84\)90061-5](https://doi.org/10.1016/0005-7967(84)90061-5)

579 45. Wolpe, J. (1969). *The practice of behavior therapy* ([1st ed.]). Pergamon Press.

580 46. Zhang, Y., Brady, M., & Smith, S. (2001). Segmentation of brain MR images through a
581 hidden Markov random field model and the expectation-maximization algorithm. *IEEE*
582 *Transactions on Medical Imaging*, 20(1), 45–57. <https://doi.org/10.1109/42.906424>

583 47. Zorowitz, S., Rockhill, A. P., Ellard, K. K., Link, K. E., Herrington, T., Pizzagalli, D. A.,
584 Widge, A. S., Deckersbach, T., & Dougherty, D. D. (2019). The Neural Basis of
585 Approach-Avoidance Conflict: A Model Based Analysis. *eNeuro*, 6(4), ENEURO.0115-
586 19.2019. <https://doi.org/10.1523/ENEURO.0115-19.2019>

587 48. Zsido, A. N. (2017). The spider and the snake – A psychometric study of two phobias
588 and insights from the Hungarian validation. *Psychiatry Research*, 257, 61–66.
589 <https://doi.org/10.1016/j.psychres.2017.07.024>

590

